Proc. IASTED International Conference on Control and Applications,
pp. 99-104, Marina del Rey, CA, USA, 2004

Control Design for a Piezo-Electric Dual-Stage Instrumented Suspension

N.K. Vestmoen Nilsen
Norwegian University of Science and Technology
Faculty of Information Technology, Mathematics and Electrical Engineering
Dept. of Engineering Cybernetics
Norway
email: nilskjet@adam.itk.ntnu.no
R.A. de Callafon
University of California, San Diego
Dept. of Mechanical and Aerospace Engineering
9500 Gilman Drive
La Jolla, CA 92093-0411, U.S.A
email: callafon@ucsd.edu

ABSTRACT
The servo control design for a piezo-electric dual-stage instrumented suspension to achieve windage vibration reduction for high track density recording is presented in this paper. The servo design exploits the information available from both the sampled position error signal (PES) and a continuous time instrumented suspension signal (ISS) available from an instrumented suspension. The ISS from the instrumented suspension is obtained by using a piezo-electric strip mounted on a dual-stage suspension to measure vibration disturbances of the suspension. Identified models were used to design an optimal fourth order continuous time servo controller to reduce track misregistration due to windage and suspension vibrations. The controller was implemented on a piezo-electric dual-stage suspension for validation purposes.

KEY WORDS
Hard disk drives, Windage, Optimal control, Weighted controller reduction

1 Introduction

One of the solutions of facilitating higher throughput data transfer has been to increase the rotational speed in a hard disk drive (HDD) [1]. Unfortunately, a higher rotational disk speed leads to more mechanical vibrations due to the windage induced suspension vibrations in the drive [2]. In addition to the windage disturbance acting on the suspension, higher requirements have been imposed on the servo system to limit track misregistration and runout errors [3, 4, 5, 6].

There are two ways of suppressing the windage induced suspension vibrations. An aero-elastic model of the flow pattern in the drive can be obtained and the housing of the drive can be redesigned such that the effect of the air turbulence on the suspension is minimized [7]. Another solution is to use active control by means of a micro-actuated suspension system [8, 9] and design a feedback control algorithm to actively dampen the windage induced vibrations on the suspension [10, 11, 12].

For the active control of the suspension vibrations, a high bandwidth feedback control system is required, as resonance modes of the suspension are in the order of several KHz. Unfortunately, the measurement of the discrete time Position Error Signal (PES) relies on the servo sectors on the disk and is limited in sampling frequency. To address the limited sampling frequency of the PES, an instrumented suspension can be used, where an additional sensor provides an high frequent or even a continuous time Instrumented Suspension Signal (ISS) that can be used for feedback purposes [8]. With the extra sensor, better control of the mechanical vibrations can be obtained

In this paper, the servo control for such a micro-actuated instrumented piezo-electric suspension is presented. The control design is based on information obtained from the windage induced disturbances that can be measured in the PES and the ISS for feedback purposes. A similar approach was taken in [11], but in this paper the control design is approached in a hybrid structure, in which the ISS is used for the design of a fast continuous time controller for windage induced vibration reduction. With the fast controller in place, the PES can be used for the design of a conventional dual-stage controller [10, 11].

2 Control Architecture

The control architecture for an instrumented and micro-actuated dual-stage suspension proposed in this paper is based on the fact that the PES is available at discrete time instances at relative low sampling frequencies (10-20kHz), while the ISS might be available at a much larger sampling

frequency or even in continuous time. Therefore, the ISS is much better suited for active high frequency vibration control due to windage excitation. As a result, a separate continuous time and a discrete time controller configured in hybrid cascade architecture are proposed in order to reduce windage induced vibrations.

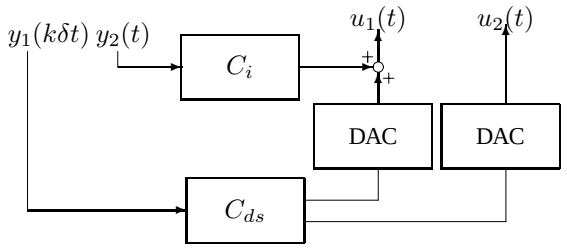

Figure 1. Hybrid control architecture with a continuous time instrumented suspension controller C_i, and a digital dual-stage controller C_{ds}.

In Figure 1 a schematic overview of the proposed hybrid control architecture is shown. A conventional discrete time sampled dual-stage controller C_{ds}, generates control signals $u_1(t)$ and $u_2(t)$ for the Voice Coil Motor (VCM) actuator and the PZT actuator on the basis of sampled PES $y_1(k\delta t)$. With the use of an instrumented suspension, a continuous or high sampling feedback controller C_i can be used for the active damping of the dual-stage suspension on the basis of the ISS $y_2(t)$. Since the controllers C_i and C_{ds} are inherently different in operation (continuous and discrete), the control design is approached separately.

The hybrid control architecture design involves two design steps. The first step consists of designing the continuous time single-input-single-output (SISO) instrumented suspension controller C_i. With the controller C_i in place, the dynamics of the suspension is changed, so as to dampen windage induced suspension vibrations. In the second step, a single-input-multiple-output (SIMO) dual-stage controller that generates control signals for both the VCM and the instrumented suspension must be designed. Both of the controllers should be designed to minimize the effect of the windage induced vibrations acting on the PES. In this paper, only the first step of the hybrid control architecture design is presented and analyzed. The second step is a standard dual-stage control problem, and several solutions already exists, see e.g [5, 8].

3 Modeling

For the control design of the instrumented suspension controller C_i, a realistic model of the instrumented dual-stage micro-actuated suspension is needed. The model should take into account the dynamics of the instrumented suspension and the windage induced vibrations as seen in the PES and ISS. In [12] it was shown that only the statistical and stochastic properties of the windage on the PES and the ISS are relevant in the servo control design for active windage suppression.

The effect of the control signal u_1 and the windage disturbance e on the PES y_1 is described by

$$y_1(t) = P_{ma}u_1(t) + H_{ma}e(t) \tag{1}$$

where P_{ma} is a models of the dynamics of the dual-stage micro-actuator (including E-block), and H_{ma} is a stable and stably invertible model of the spectral factorization of the spectral contents of the windage induced vibration disturbance as seen in the PES y_1. Similarly, the effect of the dual-stage control signal u_1 and the windage disturbance e on the ISS y_2 is described by

$$y_2(t) = P_iu_1(t) + H_ie(t) \tag{2}$$

where P_i represents a model of the dynamics of the (co-located) dual-stage instrumented suspension and H_i is a stable and stably invertible model of the spectral factorization of the spectral contents of the windage induced vibration disturbance as seen in the ISS y_2.

The model P_i in (2) is going to be used in a (negative) feedback connection

$$u_1(t) = -C_iy_2(t) \tag{3}$$

with the continuous time instrumented controller C_i. The model for H_i in (2) is used to model the windage noise disturbance as seen in the ISS $y_1(t)$, whereas the models in (1) are used to observe the effect of the windage disturbance on the PES $y_1(t)$ due to the feedback control law (3). The modeling framework is slightly different from the work in [11] as separate noise disturbance models H_{ma} and H_i are used here to take into account the presence of windage induced vibrations in the PES y_1 and the ISS y_2. The modeling of the disturbances in [11] was based on the fact that the disturbance present in the PES and ISS are the same and a low frequent sensor noise was introduced for the lack of detailed modeling of the disturbances present in the instrumented suspension signal.

A standard Prediction Error (PE) estimation technique can be used to obtain the described models of P_{ma}, H_{ma}, P_i and H_i, similar as in [13]. Based on the information obtained in the input/output data $u_1(t)$, $y_1(t)$, $y_2(t)$, $t = 1, \ldots, N$, models for P_{ma}, P_i, H_{ma}, and H_i are estimated by minimizing the prediction error

$$e_j(t, \theta_x) := H_x^{-1}(q, \theta_x)(y_j(t) - P_x(q, \theta_x)u_1(t))$$

for $x = ma$ or $x = i$ as a function of the parameters θ contained in the discrete time models $P_{ma}(q, \theta)$, $P_i(q, \theta)$, $H_{ma}(q, \theta)$, and $H_i(q, \theta)$. Parameter estimates $\hat{\theta}_x$ are obtained by minimizing the variance of the prediction error

$$\hat{\theta}_x = \min_{\theta_x} \frac{1}{N} \sum_{t=1}^{N} e_j^2(t, \theta_x)$$

Consistent estimates for $P_{ma}(q,\theta)$, $P_i(q,\theta)$, $H_{ma}(q,\theta)$, and $H_i(q,\theta)$ can be obtained when an accurate parametrization and model order is used. More details on the minimization of the PE method can be found in e.g. [13].

As in [13], the information contained in the observed input/output data $\{u_1(t), y_j(t)\}$, $t = 1,\ldots,N$, $j = 1,2$ observed over $N = 4096$ data points at a sampling time of 40kHz is used to estimate models where the resulting PE $e_j(t,\hat{\theta}_x)$ exhibits white noise characteristics to confirm consistency of the model estimates. Experimental (open-loop) data was acquired by measuring the PES with a LDV using a Hutchinson Magnum 5E suspension mounted on a E-block and connected to a VCM. The sampling rate of the PES was set at 40 kHz for modeling purposes and the rotational speed of the disk was set at 5400 RPM. To simplify the measurements and the control implementation, an open (without cover) drive was used to facilitate access of the LDV to measure PES at the outer diameter of the disk. The result of the modeling procedure is an 8th order model given in state space form:

$$\begin{aligned} \dot{x} &= Ax + Bu \\ y &= Cx + Du \end{aligned}$$

where the models (in Laplace domain) are given by

$$\begin{aligned} P_{ma}(s) &= C_1(sI-A)^{-1}B_1 \\ H_{ma}(s) &= C_1(sI-A)^{-1}B_2 + D_2 \\ P_i(s) &= C_2(sI-A)^{-1}B_3 + D_3 \\ H_i(s) &= C_2(sI-A)^{-1}B_4 + D_4 \end{aligned} \quad (4)$$

and an amplitude Bode plot of the obtained models is depicted in Figure 2.

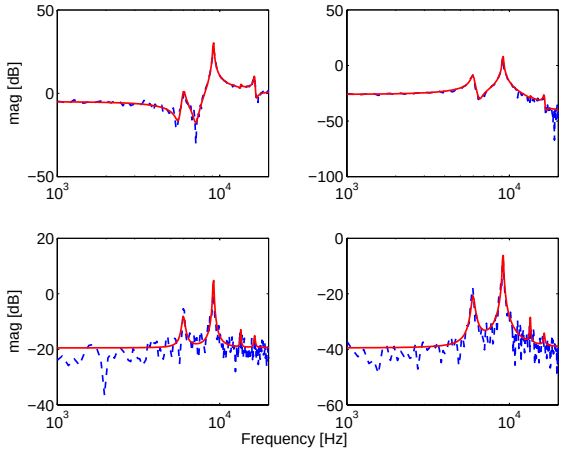

Figure 2. Amplitude Bode frequency response of spectral estimate (dashed lines) and 8th order parametric models (solid lines) of P_i (left, top), P_{ma} (right, top), H_i (left, bottom) and H_{ma} (right, bottom).

The eighth order models P_i, P_{ma}, H_i, and H_{ma} as shown in Figure 2 will form the basis for the design of the instrumented suspension controller C_i in order to reduce the vibration caused by windage disturbances.

4 Design of the Instrumented Controller

The objective of the control design is to limit the track misregistration and runout errors. The main source for the undesired movements is the windage induced vibrations, given in (1) and (2) [2]. As a first step in the hybrid design of the servo controller to minimize the windage induced vibrations, the design of the instrumented suspension controller C_i must be done on the basis of the information of the windage disturbance in the ISS and the PES signal. However, only the ISS y_2 is used for feedback purposes, as indicated in Figure 3.

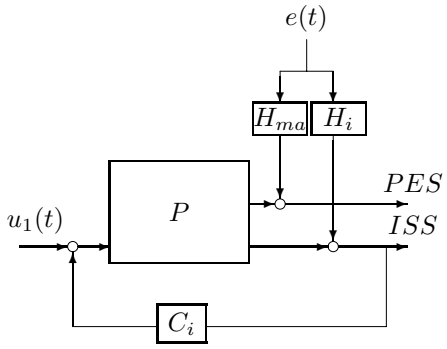

Figure 3. Design of the instrumented suspension controller C_i in the first step in the hybrid control design architecture.

The instrumented controller C_i can be described by the feedback law

$$u_1(t) = -C_i y_2(t)$$

and using the models P_i and H_i in (2) to describe the signal y_2 yields

$$u_1(t) = -C_i(P_i u_1(t) + H_i e(t))$$

making the control signal

$$u_1(t) = \frac{H_i C_i}{1 + P_i C_i} e(t)$$

Using the models P_{ma} and H_{ma} in (1), the effect of the windage induced disturbance e is the PES y_1 can be characterized by

$$y_1(t) = H_{cl} e(t),\ H_{cl} = \left[\frac{P_{ma} H_i C_i}{1 + P_i C_i} + H_{ma}\right] \quad (5)$$

In order to minimize the effect of the windage disturbance $e(t)$ on the PES y_1 with the instrumented controller C_i, the variance of y_1 can be characterized via

$$E\{y_1^2\} = \left\| H_{ma} + \frac{P_{ma} H_i C_i}{1 + C_i P_i} \right\|_2^2 \quad (6)$$

Unfortunately, minimization of (6) over C_i is not a well posed control problem and leads to high gain and possibly unstable feedback controller C_i. This is due to the fact

that the design of the instrumented controller is a co-located control problem that allows for a high gain feedback controller C_i, without jeopardizing stability of the closed-loop system of P_i ad C_i. High gain feedback is however undesirable as this requires large control signals. This can be taken into account by considering the (weighting) control signal $u_w(t) := W_u u_1(t)$ in the control design, as indicated in Figure 4.

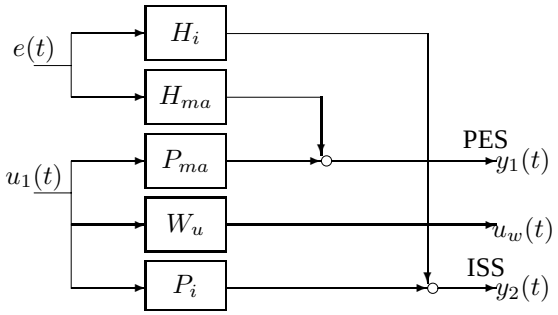

Figure 4. Block diagram of the dynamics and disturbances acting in the dual-stage suspension with a control weighting filter W_u.

With the additional weighted control signal $u_w(t) = W_u u(t)$ as a performance measure, minimizing the H_2 norm of the closed loop transfer function form e to $[y_1\ u_w]^T$ is a well-posed control design problem

$$C_i = \min_C \left\| \begin{array}{c} H_{ma} + \dfrac{P_{ma}H_iC}{1+CP_i} \\ W_u \dfrac{H_iC}{1+CP_i} \end{array} \right\|_2^2 \tag{7}$$

that can be solved using standard H_2/LQG control design techniques. For the weighting W_u a simple scalar weighting can be used, as most significant information with respect to the control design has already been captured in the model P_i, and the noise models H_i, H_{ma} and the dynamics of the instrumented suspension P_{ma}.

The resulting H_2/LQG controller from the minimization problem in (7) gives a different closed-loop performance for different choices of the scalar weighting W_u. In Figure 5 this has been demonstrated by varying W_u from 10^{-6} to 10^2 and computing the optimal controller C_i and the resulting closed-loop performance

$$\left\| H_{ma} + \frac{P_{ma}H_iC_i}{1+C_iP_i} \right\|_2^2 \tag{8}$$

It can also be noted that although all computed optimal full order controllers C_i generate a stable feedback connection with the model $P_i$of the instrumented suspension, the optimal controllers C_i for values of $W_u < 0.1$ themselves are unstable. Hence, the optimal stable full order instrumented suspension controller C_i found by choosing $W_u = 0.1$.

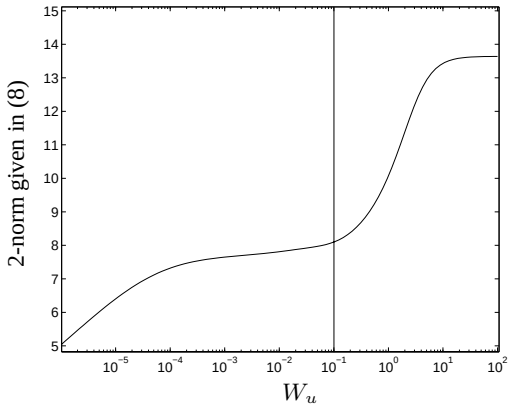

Figure 5. The closed-loop performance (8) using the optimal controller in (7) for varying values of W_u.

5 Controller Reduction

The order of the controller computed by the minimization (7) has the same order as the models P_i, P_{ma}, H_i and H_{ma} described in Section 3. In order to implement the controller, a controller reduction is required. To facilitate low order control design a direct low order control design can be done [14], but requires a non-convex optimization with possible multiple local minima. An alternative is to reduce the models P_i, P_{ma}, H_i and H_{ma} before the control design, as done in [11]. However, reducing the models can introduce modeling errors and controller designs for which stability or performance robustness cannot be guaranteed. As similar argument also holds for straightforward controller reduction based on truncation or singular perturbation of balanced state space realizations, as reduction might eliminate dynamic aspects of the controller C_i that are essential for stability or performance.

To address these problems, in the controller reduction the closed loop performance given by (8) must be preserved as much as possible. For that purpose the difference between the full order controller C_i, and a reduced order controller C_{ir} should be measured in terms of

$$H_{ma} + \frac{P_{ma}H_iC_i}{1+C_iP_i} - H_{ma} - \frac{P_{ma}H_iC_{ir}}{1+C_{ir}P_i}$$

which can be rewritten as

$$\begin{aligned} &W(C_{ir})(C_i - C_{ir}), \\ &W(C_{ir}) = \frac{P_{ma}H_i}{(1+C_iP_i)(1+C_{ir}P_i)} \end{aligned} \tag{9}$$

With these considerations in mind, the controller reduction problem can be solved as a minimization of the difference between the full order controller C_i, and a reduced order controller C_{ir} using $W(C_{ir})$ as a frequency-weighting filter.

Reduction using an iterative update of the weighting filter $W(C_{ir})$ can be done by Frequency-Weighted Balanc-

ing [15, 16] but it should be noted that (9) is still depending on W_u since C_i is a part of the minimization problem. Thus, varying W_u will give different reduced order controllers. Computation of the closed-loop performance (8) for each resulting controller in full order and reduced to 4th order designs varying W_u from 10^{-6} to 10^2 leads to the result depicted in Figure 6.

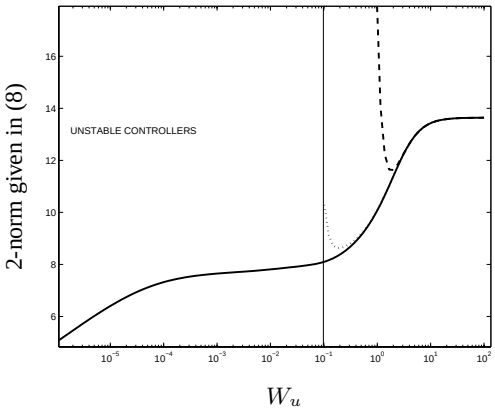

Figure 6. The closed-loop performance (8) using the optimal full order controller (solid) and reduced 4th order (weighted = dotted line, unweighted = dashed line) controllers for varying values of W_u in the range 10^{-6} to 10^2.

In Figure 6 it is worth noticing that a minimum of the closed-loop performance (8) is obtained with the frequency weighted controller reduction. The minimum with the frequency weighted reduced order controller is 8.6322 at $W_u = 0.1789$. The resulting amplitude Bode plot of closed-loop disturbance transfer function H_{cl} given in (5) for the full order C_i and frequency weighted reduced 4th order controller C_{ir} are given in Figure 7. The corresponding full order and reduced order controllers are given in Figure 8.

As seen in Figure 7, the main sway resonance mode of the suspension at 9 kHz is significantly dampened with both the full order and the reduced 4th order controller. For the resonance mode at 6 kHz not much dampening has been added, as this resonance mode has a much smaller contribution in the PES y_1 due to the windage induced vibration disturbances.

6 Experimental Results

Based on the design and analysis results, it is expected that the PES y_1 due to the windage induced vibrations will be significantly reduced since the main sway mode, which is the main component in the PES, is considerably damped by the reduced order instrumented suspension controller C_{ir}. A real-time discrete implementation of the 4th order instrumented suspension controller C_{ir} was created in a 16bit DSP environment sampled at 40kHz. A time plot of the measured PES y_1, where the control has been turned on and off is given in Figure 9 and confirms the effectiveness of the instrumented suspension controller for windage disturbance rejection, even at high frequencies.

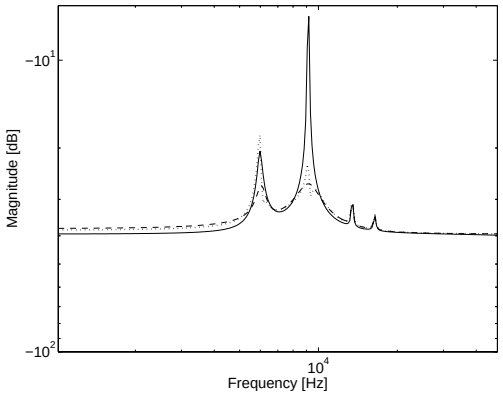

Figure 7. Open-loop disturbance transfer function H_{ma} (solid) and closed loop disturbance transfer function H_{cl} in (5) with the full order C_i (dashed) and reduced 4th order C_{ir} (dotted) instrumented suspension controllers.

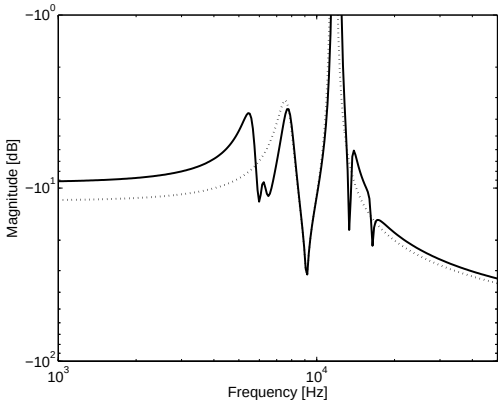

Figure 8. The full order C_i (solid) and reduced 4th order instrumented suspension controller C_{ir} (dashed).

A real-time discrete implementation of the 4th order instrumented suspension controller C_{ir}, sampled at 40kHz is given in Figure 9. As seen in Figure 9 the reduced order controller suppresses significantly the high frequent windage induced vibrations.

7 Conclusions

In this paper the servo control design for a piezo-electric dual-stage instrumented suspension to achieve windage vibration reduction for high track density recording is presented. By means of eight-order models of the dynamics describing the instrumented dual-stage suspension and the

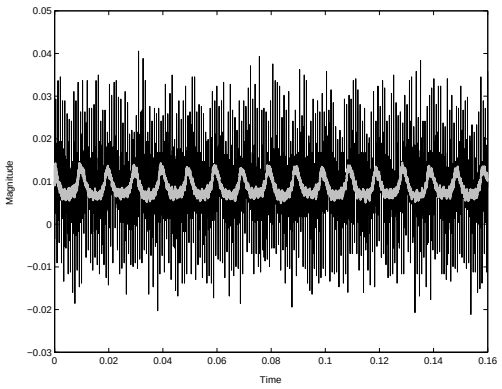

Figure 9. Time trace of the (periodic) PES y_1 with (grey line) and without (black line) control of the instrumnted suspension using the 4th order controller C_{ir}.

windage disturbances, optimal full order instrumented suspension controllers were designed to minimize the effect of windage disturbances on the position error signal. The control design is built on an architecture of a hybrid cascade controller structure in which a separation is made between the high frequent information that can be obtained from the instrumented suspension and the (relatively) low sampling of the position error signal. Reduction of controller complexity was obtained by a frequency weighted balanced reduction that takes into account the closed-loop control performance of the controller.

References

[1] H. Thapar, S.-S. Lee, C. Conroy, R. Contreras, A. Yeung, J.-G. Chern, and T. P. S.-M. Shih, "Hard disk drive read channels: Technology and trends," *Proceedings of the IEEE 1999 Custom Integrated Circuits Conference*, pp. 309–316, 1999.

[2] D. Abramovitch, T. Hurst, and D. Henze, "An overview of the PES pareto method for decomposing baseline noise sources in hard disk position error signals," *IEEE Transactions on Industrial Electronics*, vol. 34, no. 1, pp. 17–23, January 1998.

[3] N. Bando, S. Oh, and Y. Hori, "External disturbance rejection control based on identification of transfer characteristics from the acceleration sensor for access control of hard disk drive system," in *Proc. 7th Int. Workshop on Advanced Motion Control*, vol. 48, no. 5, Maribor, Slovenia, 2002, pp. 52–56.

[4] T. Goh, Z. Li, B. Chen, T. Lee, and T. Huang, "Design and implementation of a hard disk drive servo system using robust and perfect tracking approach," *IEEE Transactions on Control Systems Technology*, vol. 9, pp. 221–233, 2001.

[5] D. Horsley, D. Hernandez, R. Horowitz, A. Packard, and A. Pisano, "Closed-loop control of a microfabricated actuator for dual-stage hard disk drive servo systems," in *Proc. Of the 1998 American Control Conference*, Philadelphia, PA, USA, June 1998, pp. 3028–3032.

[6] Y. Huang, P. Mathur, and W. Messner, "Robustness analysis on a high bandwidth disk drive servo system with an instrumented suspension," in *Proc. 1999 American Control Conference*, San Diego, CA, USA, 1999, pp. 3620–3624.

[7] K. Aruga, "3.5-inch high-performance disk drives for enterprise applications: AL-7 series," *FUJITSU Sci. Tech. Journal*, vol. 37, no. 2, pp. 126–139, December 2001.

[8] Y. Li and R. Horowitz, "Mechatronics of electrostatic microactuators for computer disk drive dual-stage systems," *IEEE/ASME Transactions on Mechatronics*, vol. 6, no. 2, July 2001.

[9] M. Rotunno and R. de Callafon, "Comparison and design of servo controllers for dual-stage actuators in hard disk drives," *IEEE Transactions on Magnetics*, vol. 39, pp. 2597–2599, May 2003.

[10] M. Banther, Y. Huang, and W. Messner, "Optimal strain gauge placement for an instrumented disk drive suspension," in *Proc. 1998 American Control Conference*, Philadelphia, PA, USA, 1998, pp. 3023–3027.

[11] Y. Li, R. Horowitz, and R. Evans, "Vibration control of a PZT actuated suspension dual-stage servo system using a PZT sensor," *IEEE Transactions on Magnetics*, vol. 39, pp. 932–937, March 2003.

[12] A. Teerhuis, S. Cools, and R. de Callafon, "Reduction of flow-induced suspension vibrations in a hard disk drive by dual-stage suspension control," *IEEE Transactions on Magnetics*, vol. 39, pp. 2237–2239, 2003.

[13] M. Crowder and R. A. de Callafon, "Spectral models for windage disturbance characterization of a hard disk drive microactuator suspension," *Submitted to the Journal of Vibration and Control*, 2004.

[14] M. Rotunno and R. de Callafon, "A bundle method for solving the fixed order control problem," in *Proc. 41st IEEE Conference on Decision and Control*, Las Vegas, NV, USA, 2002, pp. 3156–3161.

[15] Y. Liu and B. Anderson, "Frequency weighted controller reduction methods and loop transfer recovery," *Automatica*, vol. 26, pp. 487–497, 1990.

[16] A. Varga and B. Anderson, "Accuracy-enhancing methods for balancing-related frequency-weighted model and controller reduction," *Automatica*, vol. 39, pp. 919–927, 21-26 July 2003.